A Marie-Curie-ITN
within H2020

*Proceedings of the International Symposium on
Thermal Effects in Gas flows In Microscale
October 24-25, 2019 – Ettlingen, Germany*

istegim2019:282778

FEMTOSECOND LASER-MICROMACHINING OF GLASS MICRO-CHIP FOR HIGH ORDER HARMONIC GENERATION IN GASES

A. G. Ciriolo[1], R. Martínez Vázquez[1*], A. Roversi[2], A. Frezzotti[3], C. Vozzi[1], R. Osellame[1,2], S. Stagira[1,2]

[1]Institute for Photonics and Nanotechnologies, National Research Council, Milan, Italy
[2]Politecnico di Milano, Physics Department, Milan, Italy
[3]Politecnico di Milano, Department of Aerospace Science and Technology, Milan, Italy
*Corresponding author: rebeca.martinez@polimi.it

KEY WORDS

Femtosecond laser micromachining, High order harmonic generation, de Laval gas micro nozzle, Attosecond science.

ABSTRACT

We report on the application of femtosecond laser micromachining to the fabrication of complex glass microdevices, for high-order harmonic generation in gas. The three-dimensional capabilities and extreme flexibility of femtosecond laser micromachining allow us to achieve accurate control of gas density inside the micrometer interaction channel. This device gives a considerable increase in harmonics generation efficiency if compared will traditional harmonic generation in gas jets. We propose different chip geometries that allow to control the gas density and driving field intensity inside the interaction channel to achieve quasi-phase matching conditions in the harmonic generation process. We believe that these glass microdevices will pave the way to future downscaling of High-order Harmonic Generation beamlines.

INTRODUCTION

Since its first observation more than twenty years ago, it is known that an intense and ultrashort laser pulse, focused in a gaseous medium, drives the emission of a burst of coherent radiation, collinear to the driving beam, with a spectral content ranging from the vacuum ultraviolet to the soft X rays [1]. This process is called High-order Harmonic Generation (HHG) since the spectrum of the emitted radiation appears as a comb of numerous odd harmonics of the fundamental laser field. In the temporal domain, this emission is structured as a train of attosecond light pulses and indeed HHG is routinely exploited in the fields of extreme ultraviolet spectroscopy and Attosecond Science [2].
Beamlines based on HHG extend over several meters since they operate in grazing incidence on bulky and expensive optics like toroidal mirrors and gratings. This instrumentation requires careful alignment and even active stabilization systems. Due to their technological complexity, HHG-based XUV (from 100 nm down to 10 nm) and soft X (from 10 nm down to 1 nm) coherent light sources are confined within a few advanced laboratories [3]. In this framework, the miniaturization of HHG beamlines will produce a substantial breakthrough in ultrafast technology, with the potential for making HHG sources available for application in numerous novel fields.
A route for achieving this breakthrough is based on femtosecond laser micromachining, which is a powerful technique that has already demonstrated its high potential in the fabrication of lab-on-chip devices [4]. Ultrashort laser pulses are focused inside a transparent sample and, due to a nonlinear absorption process, they produce a permanent modification of the material only at the focal region [5]. The basic physical mechanisms underlying this process can be outlined as follows: when a femtosecond pulse is tightly focused in a transparent

material, a nonlinear absorption mechanism, combining multiphoton and avalanche ionization, allows deposition of energy in a small volume around the focus, where the intensity is the highest [6].
The photogenerated hot-electron plasma induces high temperatures and pressures that give rise to different phenomena such as densification, direct photostructural modifications and color-center formation. Under suitable conditions, the combination of such effects may lead to a local increase of the etching speed or an increase of the refractive index of the material over a micrometer-sized volume [7]. By moving the laser focus inside the substrate one can use the laser beam to define three-dimensional regions of increased etching speed. Femtosecond Laser mIcromachining followed by Chemical Etching (FLICE) has already demonstrated its high potential in the fabrication of fused silica lab-on-a-chip devices. It can produce microfluidic networks in a 3D geometry directly buried in the glass substrate. Until now, those devices have been extensively used for the manipulation of liquids, but they are perfectly suitable for the manipulation of gases as well.
In this work, we will present gas-filled microfluidic devices, fabricated through FLICE technique, demonstrating efficient emission of extreme ultraviolet radiation produced by HHG. We exploit the flexibility, accuracy and 3D capabilities of FLICE technique to create glass microdevices for manipulating gas fluxes and for guiding laser beams through microchannels. Indeed, hollow waveguides (capillaries) are widely exploited in the field of ultrafast laser sources for the compression of intense pulses [8] and for the generation of high-order harmonics spectra up to the keV photon energy [9].

MATERIALS AND METHODS

For the femtosecond laser micromachining of the glass devices, the second harmonic (515 nm) of a femtosecond laser beam (Satsuma, Amplitude) is focused inside a fused silica sample using a 63× (0.65 NA) microscope objective (LD-plan Neofluar, Zeiss). As represented in the scheme of Fig. 1, the glass sample is mounted onto a high-resolution 3D movement system (Aerotech, ANT) and moved with respect to the laser beam following the desired trajectory. The laser repetition rate is set at 1 MHz, with a pulse duration of 320 fs and pulse energy between 200 nJ and 300 nJ depending on the dimensions of the irradiated geometry. After the laser irradiation, the sample is immersed in an ultrasonic bath of a 20% HF aqueous solution at 35°C.

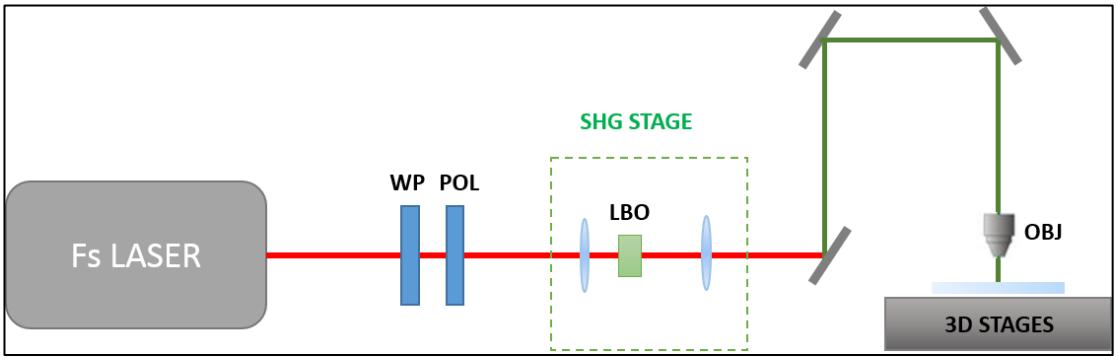

Figure 1. Femtosecond laser micromachining setup. The laser beam passes through an attenuation module, made of a λ/2 waveplate and a polarizer, and then through a telescope and a non-linear crystal (BBO) for second harmonic (515 nm) generation; the second harmonic beam is focused into the glass sample. The sample is mounted on to a 3-dimension translation stage.

HHG experiments were performed under vacuum conditions in a beamline composed of an interaction chamber (working pressure 10^{-5} mbar) and a grazing incidence XUV spectrometer (working pressure 10^{-6}-10^{-7} mbar) (see Fig. 2.). A fraction of a Ti:Sapphire laser output (25 fs, 400 μJ, 1 kHz) was focused at the entrance of the microchannel which is located inside the interaction chamber. In order to optimize the coupling with the driving laser beam, the device was mounted on a high-precision motorized alignment stage. The gas density inside the channel was accurately tuned by means of a needle valve mounted within the gas line and the gas

pressure was constantly monitored by means of a pressure gauge placed after the valve. The high-order harmonics radiation is acquired by a spectrometer composed of grazing-incidence optics. A first toroidal mirror is used for generating an intermediate focus for spectroscopy purposes. The second toroidal mirror focuses the HHG beam on a dispersion grating. The dispersed HHG signal is transduced into an electric signal by means of a Micro-Channel Plate (MCP) and the resulting electron distribution is visualized by a means of a phosphor screen. The image displayed on the phosphor screen is acquired by a CCD camera.

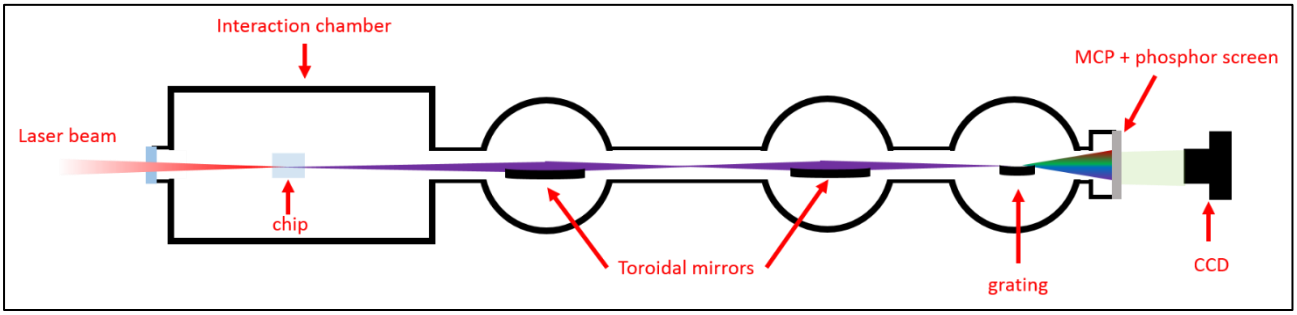

Figure 2. High-order harmonics generation and acquisition setup.

We used Comsol Multiphysics software to model the gas speed, temperature and density (in the steady-state) along the hollow waveguide. We applied the High Mach Number Flow model coupled with the so-called k-ϵ turbulence model in order to properly describe the turbulent flow behaviour of the gas inside the device. For the discretization of the geometry, we use a triangular mesh, optimized by the software from the physics of the problem. The cell dimensions vary between a maximum value of 140 μm and a minimum value of 15 μm.

RESULTS AND DISCUSSIONS

The basic design of the glass chip for HHG is shown in Fig. 3 (a); it consists of a cylindrical top central reservoir (gas pipe) from which several small microchannels (gas distribution channels) depart and reach the cylindrical horizontal main channel (hollow waveguide). The gas is inserted through the top reservoir and,

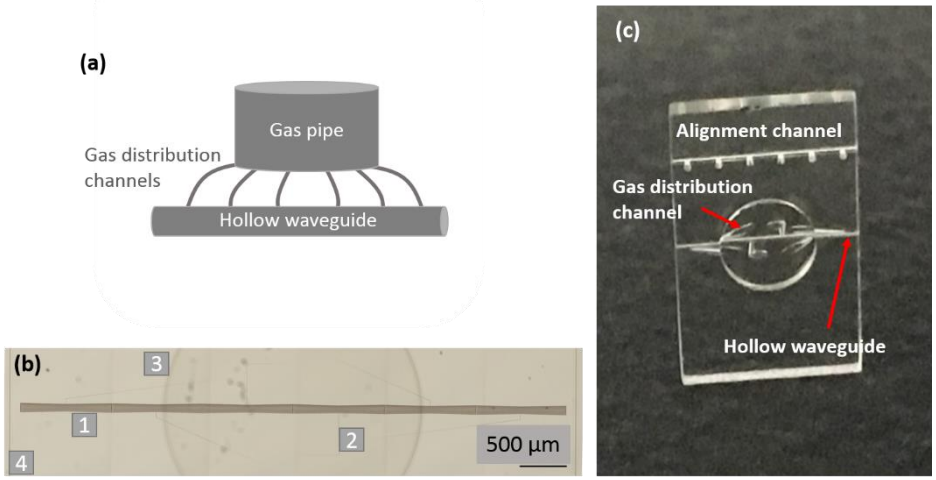

Figure 3. (a) Scheme of the HHG glass chip, (b) microscope image of the irradiated sample, the different components are evidenced: 1-hollow waveguide, 2- gas redistribution channels, 3-gas pipe reservoir, 4- lateral cutting walls, (c) picture of the device after the HF etching.

thanks to the homogeneously distributed small microchannels, it uniformly fills the hollow waveguide. In fact, the driving laser, that propagates inside the waveguide encounters a uniform gas density.

The final device is made in a fused silica plate (dimensions 6x10x1 mm) and contains two parallel microchannels; the upper one serves as an auxiliary channel for beam alignment, whereas the lower one is devoted to HHG. The reservoir for gas input has a radius of 1.6 mm, the small channels for gas distribution have variable diameter from ~100 μm (at the reservoir base) to ~30 μm at the main channel surface. The main channel, which acts as a hollow waveguide, has a 120 μm diameter. In Fig. 3 (b) and (c) are shown respectively the microscope image of the device after laser irradiation and a picture after chemical etching. The in-volume irradiated paths, which looks darker in Fig. 3(b) lead to embedded and interconnected empty channels after etching. The irradiated central channel presents a sinusoidal radius to compensate for inhomogeneous exposition to acid during the etching process, and to obtain a central channel with constant radius after the etching step (see Fig. 3(c)). It is important to point out that FLICE technique allows combining structures with millimeter size (gas reservoir with 3 mm diameter) and small structures with micrometer size (microchannels) in the same device with just one fabrication process.

To investigate the gas distribution in the microchip, we modeled the gas flow through the device in the final steady-state using Comsol Multiphysics. The results, depending on the gas backing pressure, are shown in Fig. 4. In particular, the gas temperature, density and Mach number along the capillary axis are reported. In steady conditions, the physical quantities exhibit a uniform profile within the channel. Indeed, an abrupt change in the behaviour only occurs in correspondence of the exits towards the vacuum chamber, where the gas undergoes a remarkable acceleration.

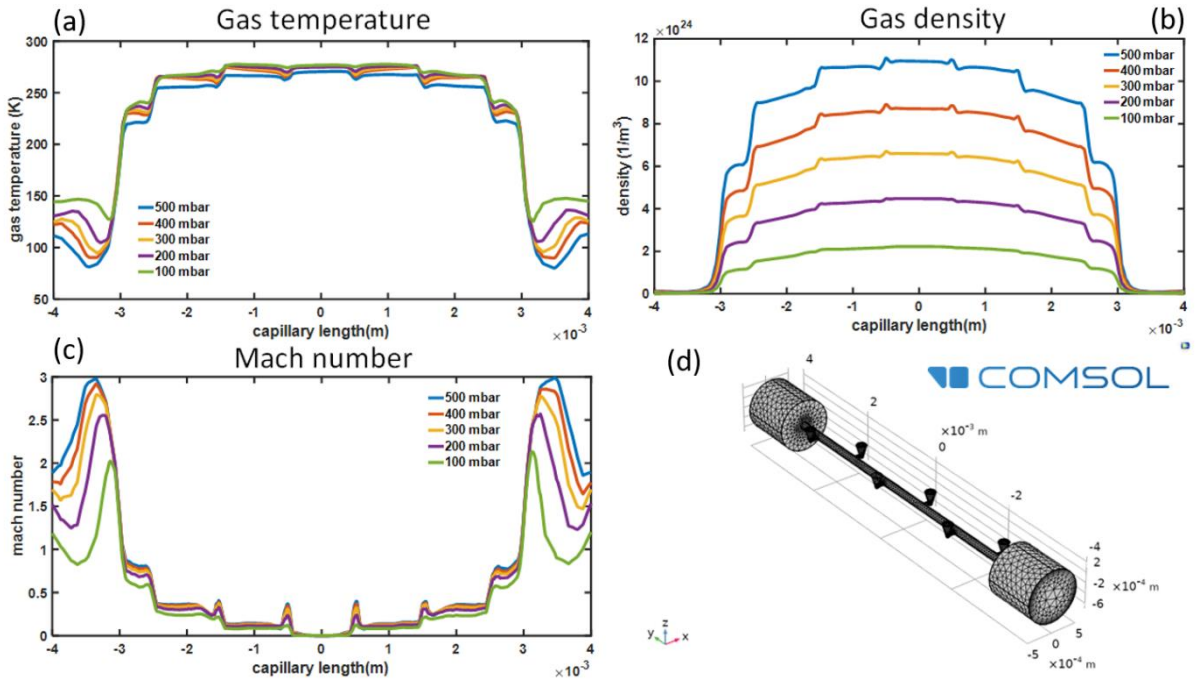

Figure 4. Numerical simulation of the gas evolution inside the micromachined device reported in Fig. 2, showing (a) gas temperature, (b) density and (c) Mach number as a function of the gas backing pressure. (d) Gas volume geometry and mesh. The main channel and the small lateral features reproduce the chip internal structure. The two cylindrical structures placed at the extremities are used as output volume for simulating gas expansion in the interaction chamber. The simulations were performed using COMSOL.

The gas density inside the channel scales linearly with the backing pressure. Thus, by properly monitoring the backing pressure, it is possible to achieve accurate control of the density of the generating medium inside the microchannel and, as a consequence, of the generated harmonics intensity.

For the HHG experiments the gas pipe was connected to the glass chip which is positioned into the interaction chamber and the laser beam was coupled inside the hollow waveguide. Fig. 5(a) shows a comparison among different harmonic spectra generated inside the microchannel filled with neon gas. A decreasing yield was observed when the gas backing pressure was increased from 50 to 210 mbar. The reduction is more evident for low-order harmonics, as indicated by the reshaping of the harmonic spectrum. This pressure dependence is due to both phase-matching effects and absorption from the gas: as the pressure increases, the XUV radiation is strongly absorbed; moreover, the phase mismatch between the fundamental and the harmonic field worsens and leads to a dramatic reduction of the yield mainly in the low-energy part of the spectrum [10,11].

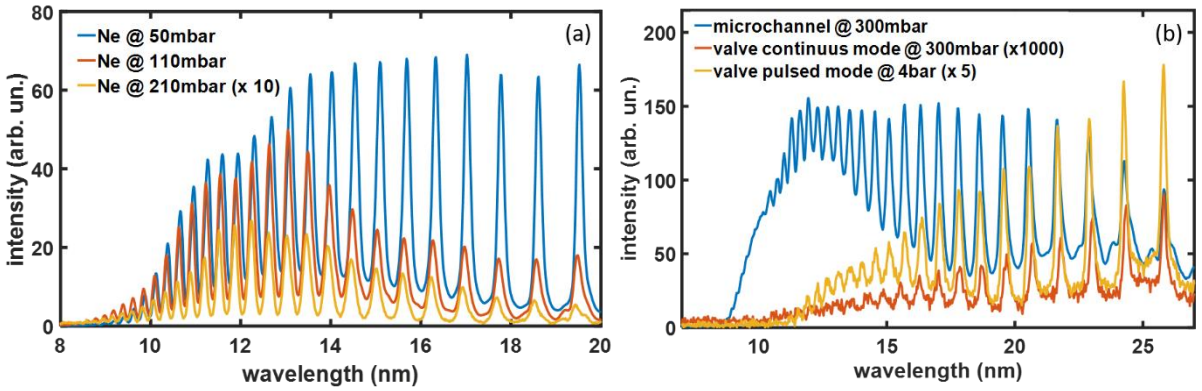

Figure 5. (a) HHG spectra generated inside the chip using Neon gas with a backing pressure of 50 (blue), 110 (red) and 210 mbar (yellow); this latter curve is magnified 10 times. (b) Comparison between HHG spectra produced in helium inside the microchannel (blue), in a continuous gas jet (red) and in a pulsed gas jet (yellow).

We compared the optimal HHG yield inside the channel filled with helium gas with that achieved in the most commonly used interaction geometry based on a helium gas jet. Figure 5(b) shows single-shot harmonics spectra generated inside the channel with helium at a 300-mbar backing pressure (blue line). The results are compared to HHG in a steady helium jet with 1 mm diameter at the same gas pressure (red line, x1000 magnification) and in a pulsed jet with the same diameter at a 4-bar backing pressure (yellow line, x5 magnification). An extended cutoff, up to 7 nm (160 eV) is obtained inside the microchannel, whereas a cutoff of about 11 nm (110 eV) is observed in the jets. Moreover, a higher generation yield is achieved in the microchannel, up to 20 times the pulsed jet and about 10^4 times the steady one. The improved performances achieved in the microchannel are related both to the extension of the interaction region and the different interaction geometry with respect to the gas jets.

Although there is an overall improvement in the generation yield with respect to traditional HHG in gas we are confident that a further improvement in the harmonic generation can be obtained by overcoming the phase-matching limitations. In fact, as in many nonlinear processes, HHG efficiency depends both on the single-atom response [12] and on the macroscopic response during propagation in the medium [13], so for generating a bright output beam the emission of a large number of atoms over an extended region must add in phase. The phase relationship between the fundamental and the harmonics field depends on several factors, that are mainly related to the generating medium and the generation geometry. In particular, the gas neutral and free-electron plasma optical dispersion is wavelength-dependent, so that the fundamental field and the newly generated harmonics can accumulate a phase-mismatch during the propagation. The geometrical phase effects depend instead on the space-structure of the fundamental beam, either tight-focusing or waveguide-assisted confinement.

Practical approaches exploiting Quasi Phase-Matching (QPM) are challenging [9]. In this sense, we are modeling and prototyping different microchip for HHG endowed with multiple gas micro-jets, with the attempt of exploiting QPM. We are following two main strategies which are known to be effective in the improvement of the HHG yield, i.e. the modulation of the driving field intensity or the modulation of the gas density [14,15]. Modulation of the driving field intensity is achievable through modulation of the hollow waveguide diameter. In fact the diameter of the propagating mode will depend on the waveguide diameter and as a consequence also the peak intensity [16]. In Fig. 6, panels (a) and (b) we show the scheme and microscope image of the microchip with the modulated radius. The gas delivery inside the channel is similar to the one in the previous device; it is inserted through the top reservoir, flows through a network of microchannels and reaches the hollow waveguides at some specific positions. In addition, in this device each delivering microchannel faces a small exit channel in order to create a modulation of gas density. The strong capabilities of FLICE technique are evidenced in this glass which has a 20% radius modulation (110 μm-135 μm) and 30 small gas inlets and outlets with micrometer size.

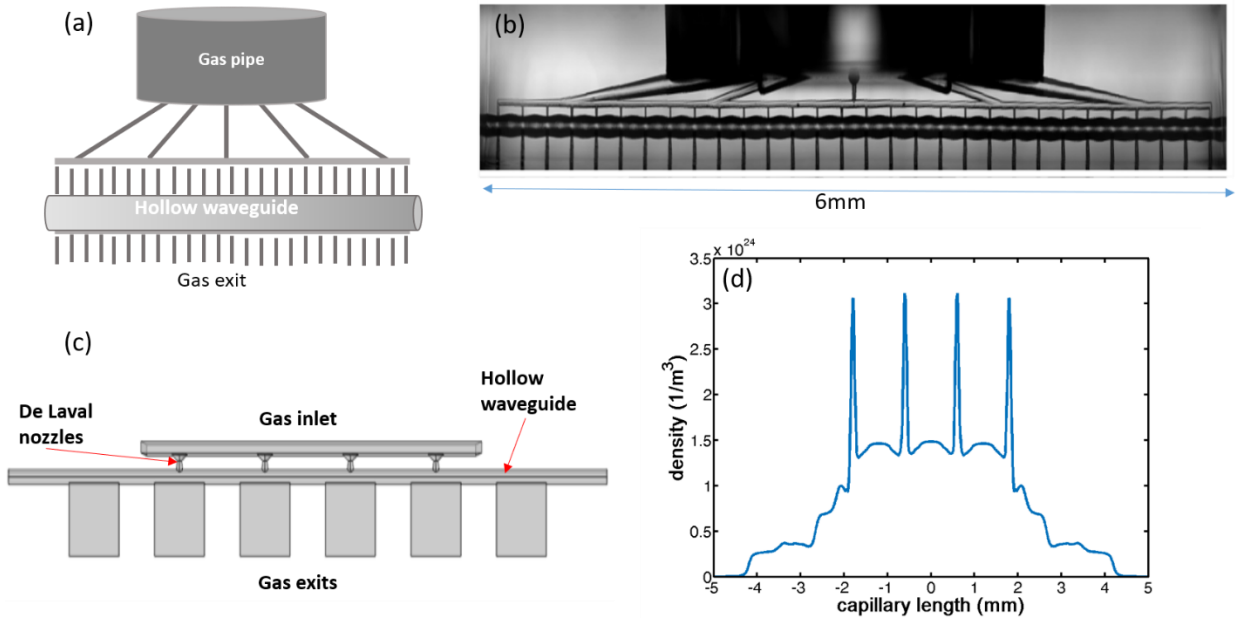

Figure 6. (a) Cartoon of the quasi phase matching device with 32 gas inlet and modulated diameter (b) microscope image of the device in (a). (c) Cartoon of the device with the supersonic gas jets created by micro-nozzles. (d) Comsol numerical simulation of gas density(Ne) inside the chip shown in (c), with 1bar backing pressure.

It is possible to achieve an even higher modulation of the gas density inside the hollow waveguide by injecting the gas through a series of de Laval micro-nozzles whose supersonic flow condition, at the end of the divergent section, helps producing a more focused gas jet. The scheme of the chip is shown in Fig. 6 (c), in this device, there is no gas reservoir and the convergent section of each nozzle is almost directly facing the gas inlet. Different nozzle geometries were numerically investigated, using Comsol software, in order to enhance/control the density modulation along the axis of the hollow waveguide.

It should be noticed that the nozzle flow behavior in the considered conditions deviates from the classical one, as described by inviscid theory. Although the inlet pressure is high enough to avoid rarefaction effects, viscous forces are very pronounced (the nozzle throat Reynold's number is about 300) and delay the supersonic transition within the divergent section whose effective area is strongly reduced by a thick boundary layer [17]. So far, the best nozzle configuration consists of a simple double cone geometry with an inlet diameter of 220 μm, a 60 μm throat diameter and a 90 μm exit diameter, whose size is the largest possible which preserves the guiding characteristics of the hollow waveguide. The overall nozzle length is 131 μm. Fig. 6 (d)) shows the simulated gas density profile along the waveguide axis. A strong density increase in correspondence with the nozzle position is clearly visible and expected to be high enough to obtain QPM.
Due to these two strategies that can be implemented in microchips – either separated or together - we expect to obtain HHG in a Quasi-Phase Matching (QPM) regime [14,15] that would boost the generation yield by 1-2 orders of magnitude with respect to the already good performance of the first-generation devices. We are performing computational simulations of the harmonic generation process upon QPM in order to optimize the periodicity of the gas jet and of the channel modulation.

CONCLUSIONS

In the present work, we have demonstrated the application of femtosecond laser micromachined glass microchips to the generation of high-order harmonics in gas. The working principle relays in a main cylindrical microchannel that acts as a hollow waveguide where the driving laser propagates. This microchannel is filled with gas through a three-dimensional network of gas distribution channels all embedded in the glass device. The gas flow has been numerically studied and characterized. As a result of the laser-gas interaction, an increase of the HHG signal was observed, which surpasses the performances of the standard generation configuration based on pulsed gas-jets both in terms of efficiency and spectral extension.
By exploiting the extreme flexibility of the FLICE technique, different generation prototypes including gas-micro-jets and periodically structured capillaries, have also been realized, aiming at further improving the HHG efficiency in a Quasi Phase-Matching regime.
We foresee that the FLICE technique can be exploited to downscale an entire HHG-based beamline to a glass chip, integrating several additional functionalities like the separation of the IR driving beam from the HHG radiation by waveguide effects, and the inclusion of an interaction module for HHG spectroscopy in liquid and gaseous samples. The realization of an attosecond lab-on-chip can be envisioned in the long-term.

AKNOWLEDGEMENTS

This study was supported by the European Union's Horizon 2020 research and innovation program under the Marie Skłodowska-Curie projects ASPIRE (Grant No. 674960), by the European Research Council Starting Research Grant UDYNI (Grant No. 307964), by the Italian Ministry of Research and Education (ELI project – ESFRI Roadmap).

REFERENCES

[1] Kraus, F., & Ivanov, M. (2009). Attosecond physics. *Rev. Mod. Phys.* **81**, 163-234.
[2] Calegari, F., Sansone, G., Stagira, S., Vozzi, C., & Nisoli, C. (2016). Advances in attosecond science. *J. Phys. B: At. Mol. Opt. Phys.* **49**, 062001.
[3] Kühn, S., et al. (2017). The ELI-ALPS facility: the next generation of attosecond sources. *J. Phys. B: At. Mol. Opt. Phys.* **50**, 132002.

[4] Sima. F., Sugioka, K., Martínez Vázquez, R., Osellame, R., Kelemen, L., & Ormos, P. (2018). Three-dimensional femtosecond laser processing for lab-on-a-chip applications. *Nanophotonics* **7**, 613-634.
[5] Gattass, R. R., & Mazur, E. (2008). Femtosecond laser micromachining in transparent materials. *Nature Photonics* **2**, 219-225.
[6] Davis, K.M., Miura, K., Sugimoto, N., & Hirao, K. (1996). Writing waveguides in glass with a femtosecond laser. *Opt. Lett.* **21**, 1729-1731.
[7] Marcinkevičius, A., Juodkazis, S., Watanabe, M., Miwa, M., Matsuo, S., Misawa, H., & Nishii, J. (2001). Femtosecond laser-assisted three-dimensional microfabrication in silica. *Opt. Lett.* **26**, 277-279.
[8] Nisoli, M., Stagira, S., De Silvestri, S., Svelto, O., Sartania, S., Cheng, Z., Tempea, G., Spielmann, C., & Krausz, F. (1998). Toward a Terawatt-Scale Sub-10-fs Laser Technology. *IEEE JSTQE* **4**, 414-420.
[9] Popmintchev, T., & et al. (2012). Bright coherent ultrahigh harmonics in the keV x-ray regime from mid-infrared femtosecond lasers. *Science* **336**, 1287-1291.
[10] Ciriolo, A. G., & et al. High-order Harmonic Generation in Femtosecond laser-Micromachined Device. *Conference on Lasers and Electro-Optics 2018 (CLEO 2018)*, San Jose, California, United States.
[11] Martínez Vázquez, R., & et al. (2019). Femtosecond laser micromachining of glass chips for High-order Harmonic Generation. Photonics West 2019, San Francisco, California, United States.
[12] Corkum, P.B.(1993). Plasma Perspective on Strong-Field Multiphoton Ionization. *Phys. Rev. Lett.* **71**, 1994-1997.
[13] Reintjes, F. (1984). Non-Linear Optical Parametric Processes in Liquid and Gases. Academic Press, New York.
[14] Gibson, E., & et al. (2003). Coherent Soft X-ray Generation in the Water Window with Quasi-Phase Matching. *Science* **302**, 95-98.
[15] Pirri, A., Corsi, C., & Bellini, M. (2008). Enhancing the yield of high-order harmonics with an array of gas jets. *Phys Rev A* **78**, 011801R.
[16] Marcatili, E. A. J., & Schmeltzer, R.A. (1964). Hollow Metallic and Dielectric Waveguides for Long Distance Optical Transmission and Lasers. *Bell System Technical Journal* **43**, 1783-1809.